Multielectron structure and dynamics in scaled-energy Stark photoabsorption and recurrence spectra

J. D. Wright, H. Flores-Rueda, W. Huang, and T. J. Morgan
Department of Physics, Wesleyan University, Middletown, Connecticut 06459, USA
(Received 26 April 2008; revised manuscript received 19 February 2009; published 15 May 2009)

We use the $4s[3/2]_2^o$ metastable state of atomic argon created by charge-transfer collisions between a 5 keV Ar^+ beam and K vapor to perform laser scaled-energy Stark photoabsorption and recurrence spectroscopy of even-parity Rydberg states, detected by field ionization and forced autoionization, in a region of the spectrum that contains two distinct perturbations. We apply a uniform electric field that changes with the frequency of the laser to maintain a constant scaled energy relative to the first ionization limit of the atom, associated with the ion core in a $^2P_{3/2}$ configuration. Local perturbations to the Rydberg series ($15 \leq n \leq 28$) occur due to $n'=8$ and 10 Stark states that belong to the series converging to the second ionization threshold with the ion core in a $^2P_{1/2}$ configuration. The resulting absorption spectra show multielectron effects due to configuration interaction and angular momentum coupling. These effects have dynamical implications in the recurrence spectrum. In particular, the variations in the Stark structure of the absorption spectrum result in a recurrence spectrum that shows two prominent multielectron features. One is the presence of recurrence peaks with scaled actions less than that of the hydrogenic primitive orbit. We attribute this to excitation in which both the ion core and the Rydberg electron absorb energy during photoexcitation. The second multielectron effect observed is recurrence peaks that occur at the sum of scaled actions of the primitive orbit (and its repetitions) associated with the pair of perturbations and a hydrogenic closed classical orbit. We attribute these peaks to core-changing inelastic scattering of the Rydberg electron with the ionic core due to angular momentum coupling. For comparison, we measured the regular autoionizing Rydberg series of argon between the first and second ionization thresholds, where no perturbing resonances exist.

DOI: 10.1103/PhysRevA.79.052510 PACS number(s): 32.30.Jc, 05.45.Mt, 32.60.+i, 32.80.Ee

I. INTRODUCTION

One method of investigating the semiclassical dynamics of atoms in external fields is frequency-domain recurrence spectroscopy [1–3]. To perform Stark scaled-energy spectroscopy of atoms, the electric-field strength F changes with the electron binding energy E to maintain a constant scaled energy $\varepsilon = EF^{-1/2}$ and a classically invariant scaled Hamiltonian. Since the scaled Hamiltonian does not depend independently of the binding energy and applied field, a photoabsorption spectrum recorded at a particular scaled energy ε maintains the classical dynamics of the system constant, and its Fourier transform with respect to the effective principal quantum number $n^* = (2E)^{-1/2}$, the recurrence spectrum, contains peaks at scaled actions S', associated with electron motion that periodically closes at the atomic core [1–5].

Throughout the last decade, several experimental studies were undertaken on the structure of the Stark recurrence spectrum in atomic systems that exhibit a regular one-electron Rydberg series [5–10] and, consequently, the spectrum is well understood in an unperturbed atomic system [11]. However, the effects of perturbing states on the recurrence spectrum of atomic systems is much less understood and investigated.

We are aware of only two published experimental studies of perturbed Rydberg atoms in electric fields using frequency-domain recurrence spectroscopy. The first study in 2001 by Bates *et al.* [12] analyzed recurrence spectra of barium Rydberg atoms in a static electric field where several singly excited Rydberg states were perturbed by one doubly excited electronic state. This strong perturbation in the photoabsorption spectrum creates an energy-dependent quantum defect for the singly excited Rydberg series and shifts the positions of the recurrences peaks relative to those of a one-electron atom [12]. In 2007, Murray-Krezan *et al.* [13] performed scaled-energy spectroscopy of Rydberg atoms in a static electric field using an excitation scheme that permitted the observation of both perturbed and unperturbed regions in the photoabsorption spectra of barium and calcium. A comparison between recurrence spectra associated with perturbed and unperturbed regions of the photoabsorption spectra led to the identification of not only shifting but also splitting of recurrence peaks that were associated with two-electron dynamics. In both studies, each spectrum contained only one perturbing state.

In the present work, we extend these studies by examining a region of the photoabsorption spectrum of argon that con-

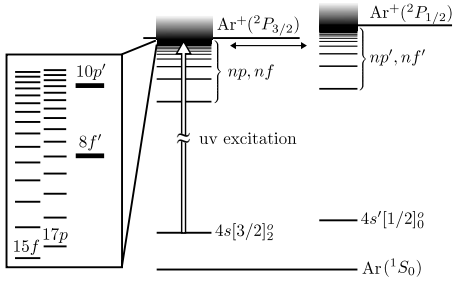

FIG. 1. Experimental excitation scheme and energy-level diagram for the argon atom in zero field. The double-sided horizontal arrow indicates the region of overlap between the np, nf and np', nf' Rydberg series investigated in the present study and magnified in the inset portion of the figure.

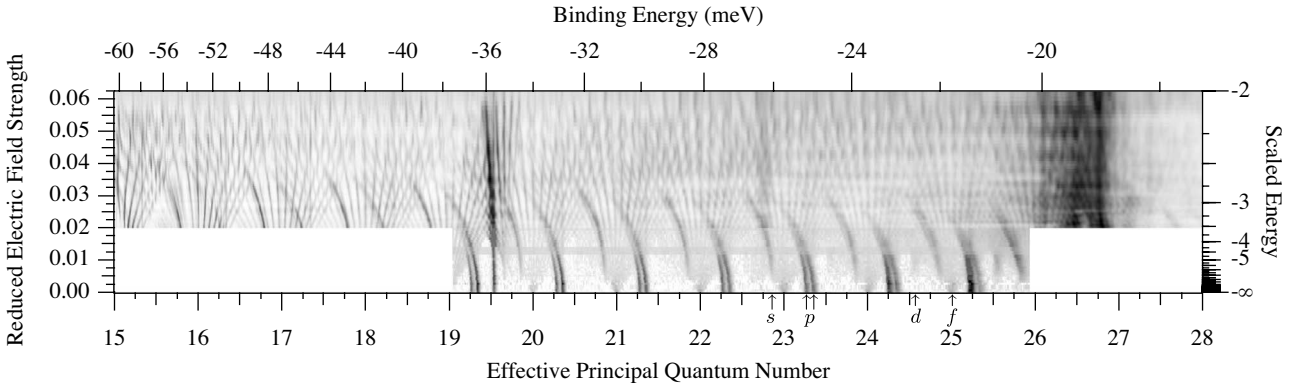

FIG. 2. Measured Stark photoabsorption map of argon consisting of 66 individual spectra as a function of reduced electric-field strength $1/4\varepsilon^2$ and effective principal quantum number. The right ordinate is scaled energy. Upper abscissa is binding energy in meV measured relative to the $^2P_{3/2}$ ionization threshold. Black and white represent high and low photoabsorption intensities, respectively. Two perturbations in the repeating structure are present at n^* values of 19.6 and 26.6. Data were not collected in the blank regions. The arrows along the bottom axis point to the zero-field locations of the $n=25$ s, p, d, and f Rydberg states.

tains two distinct perturbations. This introduces new frequencies in the recurrence spectrum and consequently in addition to splitting and shifting of recurrence peaks, new peaks emerge in the spectrum. We associate the new peaks in the measured Stark recurrence spectrum with core-changing collisions due to the multielectron dynamics of the Rydberg electron and an open-shell ion core.

We investigate the Rydberg states ($n=15-28$) that converge to the first continuum for which the ion core occupies a $3p^5(^2P_{3/2})$ state. The spectrum contains interloper states ($n'=8$ and 10) associated with another Rydberg series that converges to a second continuum for which the ion core resides in a $3p^5(^2P_{1/2})$ state [14]. Figure 1 shows the relevant energy diagram for zero electric field. The initial $4s[3/2]_2^o$ metastable state contains both s and d components for the orbital angular momentum of the valence electron as well as both 1/2 and 3/2 components for the total angular momentum of the ion core. Consequently, np, nf, np', and nf' final states carry intensity when excitation occurs in zero field. These final states are actually multiplets containing many unresolved fine-structure components so that electric dipole transitions from the $4s[3/2]_2^o$ metastable state in zero electric field access the $np[1/2]_1$, $np[3/2]_1$, $np[3/2]_2$, $np[5/2]_2$, $np[5/2]_3$, $nf[3/2]_1$, $nf[3/2]_2$, $nf[5/2]_2$, $nf[5/2]_3$, and $nf[7/2]_3$ fine-structure components of the $^2P_{3/2}$ Rydberg series and the $10p'[1/2]_1$, $10p'[3/2]_2$, $10p'[3/2]_2$, $8f'[5/2]_2$, $8f'[5/2]_3$, and $8f'[7/2]_3$ fine-structure components of the $^2P_{1/2}$ Rydberg series. A uniform static electric field mixes these different channels. Methods using multichannel quantum-defect theory (MQDT) and configuration interaction successfully describe photoabsorption spectra of multielectron atoms, and here we consider how MQDT and configuration-interaction effects are reflected in the Stark recurrence spectrum.

II. EXPERIMENT

A. Procedure

The experimental apparatus and procedures are similar to that previously discussed in our studies of atomic helium and argon in electric fields [10,15] and will be only briefly described here. The experiment consists of measuring a scaled-energy absorption spectrum and performing the appropriate Fourier transform to obtain the recurrence spectrum. In the present case, we use the $4s[3/2]_2^o$ metastable state of argon created in a fast-beam machine (5 keV, 10^{-6} torr) to perform classically scaled photoabsorption and recurrence spectroscopy of even-parity Rydberg states of atomic argon in a uniform electric field. The metastable states are formed by

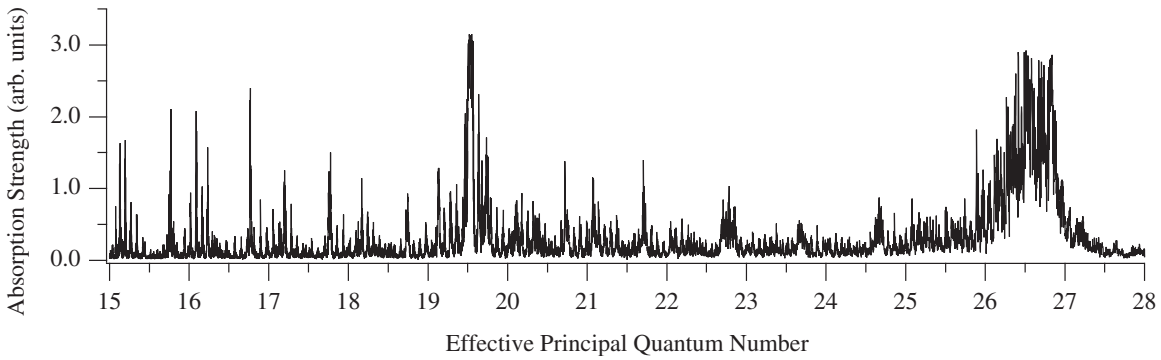

FIG. 3. Measured photoabsorption spectrum of argon at scaled energy $\varepsilon=-3.175$ over the range of $n^*=15-28$. The two large-scale features in the spectrum at $n^*\sim 19.6$ and ~ 26.6 are caused by the $n'=8$ and 10 perturbers, respectively.

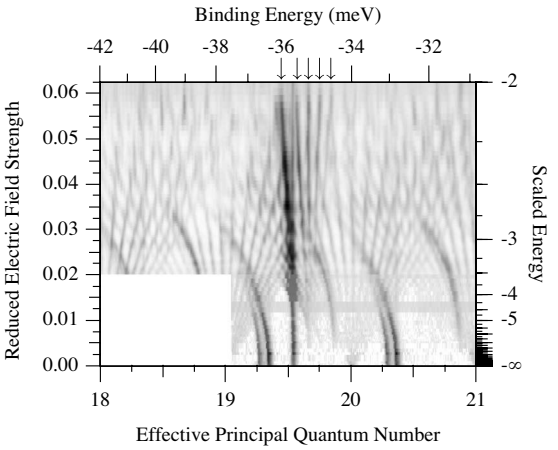

FIG. 4. Measured Stark photoabsorption map of argon over three effective principal quantum numbers in the vicinity of the $8f'$ perturbation.

electron-capture collisions of argon ions in a potassium vapor cell. After the cell, the metastable atoms are excited to Rydberg states by a counterpropagating collinear 20 Hz laser beam (bandwidth, 0.22 cm^{-1}) over an interaction path length of 40 cm that resides inside a pair of parallel metal plates to which a voltage is applied to provide a Stark field transverse to the beam. Downstream from the interaction region, the Rydberg atoms pass through a longitudinal 7 kV/cm ionizing electric field. This field ionizes Rydberg states with principal quantum number $n \geq 12$ and induces forced autoionization of Rydberg states with $n' > 7$ [16]. The resulting ions are electrostatically analyzed and steered into a channeltron whose output is amplified, shaped, and boxcar averaged for data accumulation. The laser wave number is calibrated using a field-free spectrum of argon. The range of photoexcitation is 33 736–34 200 cm^{-1}. The relative energy scale of the experimental photoabsorption spectrum has an estimated uncertainty of 0.1 cm^{-1}, established by frequency markers from an etalon with free spectral range of 0.7 cm^{-1}.

B. Observations of Stark absorption spectra

Figure 2 shows the measured Stark absorption map of argon (the compilation of 66 spectra taken at different scaled energies measured relative to the $^2P_{3/2}$ ionization limit) for laser polarization parallel to the applied electric field. The vertical scale is a linear function of the reduced electric-field strength [17] F_r, which directly relates to the square of the scaled energy as

$$F_r = \frac{1}{4\varepsilon^2}. \tag{1}$$

Figure 2 uses a linear scale of reduced field along the left ordinate in order to compactly display the entire measured Stark map, from zero electric field ($F_r=0$ or $\varepsilon=-\infty$) to the classical electric-field-ionization limit ($F_r=0.0625$ or $\varepsilon=-2$). The right ordinate displays a nonlinear scale of scaled energy. The bottom abscissa displays a linear scale of effective principal quantum number, which serves as the Fourier transform variable used to obtain the recurrence spectrum and ranges from 15 to 28. The top abscissa displays the binding energy measured relative to the first ionization limit on a nonlinear scale. The grayscale intensity represents the photoabsorption intensity, with smaller intensities being closer to white and greater intensities being closer to black. The data were taken in two different experimental runs. Data were not collected in the empty regions of the map.

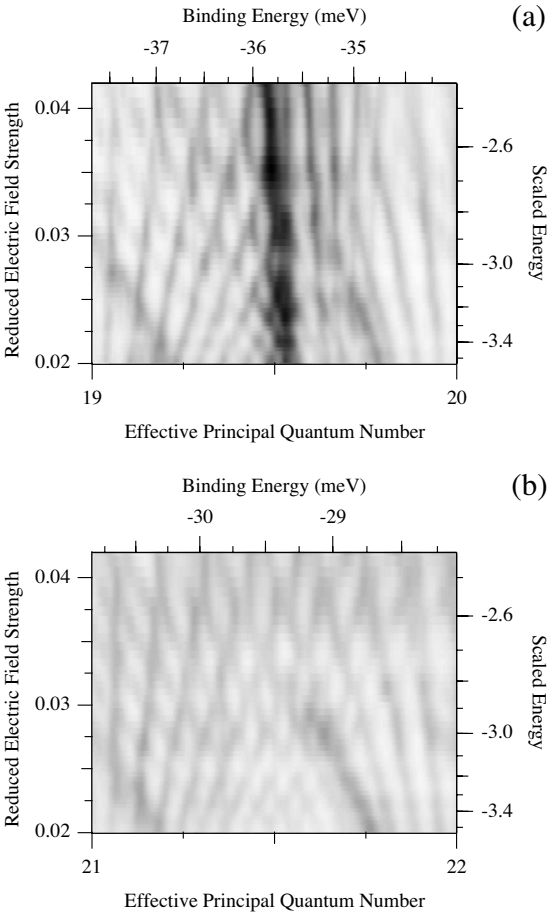

FIG. 5. Zoomed-in view of the measured Stark photoabsorption map of argon over one effective principal quantum number with (a) $n^*=19$ and 20 and (b) $n^*=21$ and 22.

The map contains clear perturbed and unperturbed regions. The two irregular features in the map at n^* values of $\sim$19.6 and $\sim$26.6 are caused by the $n'=8$ and 10 perturbations, respectively, which occur at a scaled energy relative to the $^2P_{1/2}$ ionization limit ε' of $(n^*/n^{*\prime})^2\varepsilon$ [18]. (An additional low-intensity nonregular region is seen in the map at $n^* \sim 22.8$ and is not identified.) Figure 3 shows the $\varepsilon=-3.175$ scan to illustrate the behavior of a single spectrum in the map.

The Rydberg states with a $3p^5(^2P_{3/2})$ ion core are detected by field ionization, while the Rydberg states with a $3p^5(^2P_{1/2})$ ion core are detected by forced autoionization [16] made energetically possible by the electric-field-induced depression in the $^2P_{3/2}$ ionization potential.

The unperturbed regions of the map contain numerous Stark states with regular hydrogenic manifolds associated with the ion core in its ground-state configuration,

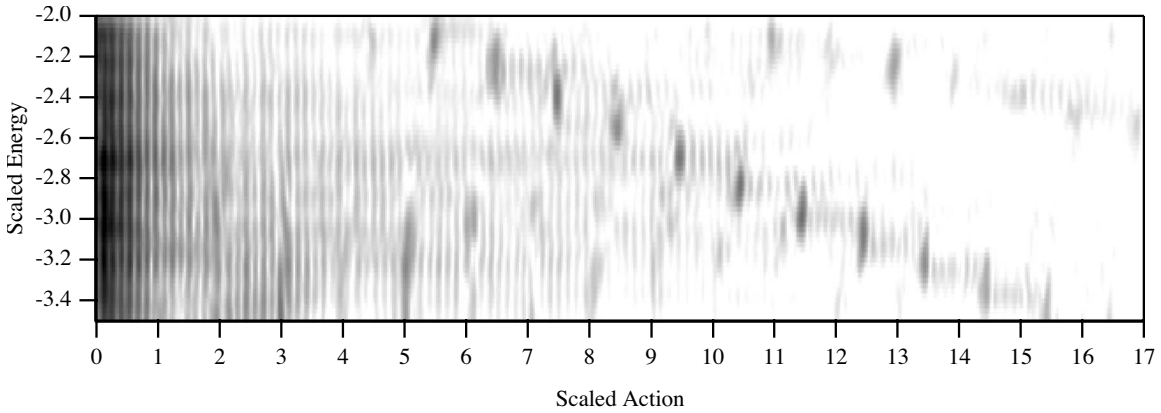

FIG. 6. Measured Stark recurrence map of argon as a function of scaled energy ε and scaled action S'. Black and white areas represent high and low recurrence strengths, respectively. The two structures cutting diagonally through the map are the first and second bands of closed classical orbits [10].

$3p^5(^2P_{3/2})$. With the present experimental resolution and field-free conditions, we observe the dipole-allowed np and nf states, which appear as doublets and singlets, respectively, with most of the intensity in the np states. (The zero-field locations of the s, p, d, and f states nearest to $n^*=25$ are identified by arrows in Fig. 2.) For nonzero electric fields the nf states with a small quantum defect ($\delta_f \sim -0.01$) evolve into the linear Stark manifold and the np states with a larger quantum defect ($\delta_p \sim -1.7$) exhibit a quadratic Stark effect. The ns states ($\delta_s \sim -2.1$) evolve into Stark states that emerge at a reduced field of approximately 0.006 and also exhibit a quadratic Stark effect as can be seen in Fig. 2. The Stark state that evolves from the $26d$ state can also be seen in Fig. 2 in the vicinity of $n^*=25$.

The broad feature in the vicinity of $n^*=26.6$ results from the Stark manifold of states that evolves from the $10p'$ manifold of fine-structure components. Over the measured range of scaled energies, $\varepsilon=-3.5$ to -2, the $10p'$ manifold experiences a range of scaled energies relative to the $^2P_{1/2}$ ionization limit, $\varepsilon'=-21.2$ to -37, that corresponds to essentially zero field. In zero field, the $10p'$ perturber consists primarily of the $10p'[1/2]_1$ state with a small contribution from the $10p'[3/2]_1$ state, based on a recent analysis of the neighboring $11p'$ multiplet [19,20]. The effects of the perturber can be clearly seen in Fig. 2. This perturbation visibly interacts with the underlying Rydberg series. The main effect of the perturber on the underlying Rydberg series is to enhance (diminish) the oscillator strengths of the series toward lower (higher) energies. This feature is much broader than the second perturbed feature in the map at $n^*=19.6$ because the $10p'$ state has lower angular momentum than the $8f'$ state and also because the spectrum is plotted versus n^* rather than E.

At zero field the spectral feature around $n^*=19.6$ results from the $8f'$ manifold of fine-structure components. The manifold consists of $8f'[5/2]_3$ with a small contribution from $8f'[5/2]_2$, based on a recent analysis of the neighboring $9f'$ multiplet [20] and experiences negligible interaction with neighboring states at zero field [21]. At nonzero fields the $8f'$ manifold evolves into a manifold of Stark states and interacts with the underlying Stark Rydberg series. Within the $n'=8$ Stark manifold there are five states that evolve from the zero-field $8f'$, $8g'$, $8h'$, $8i'$, and $8k'$ states, all of which can be clearly seen in Fig. 4 and are identified by arrows. (The other three Stark states in the $n'=8$ manifold that evolve from the field-free $8s'$, $8p'$, and $8d'$ states are all shifted far from the manifold due to their large quantum defects). A low-intensity unshifted line is also present as a result of excitation in zero-field regions of the apparatus.

Close inspection of the feature around $n^*=19.6$ in Fig. 4 or 5(a) shows three distinct areas: an area of relatively intense absorption to the lower-n^* side, an area of Stark structure of the $n'=8$ states (for this case ε' ranges from -11 to -19.3, in the Stark bowtie region [16], the region of a Stark map where the extremal spectral lines in adjacent Stark manifolds have not yet overlapped, and an area of diminished absorption intensity to the higher-n^* side. Also, the $8f'$ Stark structure noticeably interacts with other Stark states from the $^2P_{3/2}$ channel that shift into its path. For instance, for reduced fields greater than ~ 0.02, in the region between $n^*=19$ and 19.5, the $n'=8$ manifold mixes with several red-seeking (blue-seeking) states at the edge of the $n=20$ (19) Stark manifold, increasing their absorption relative to the unperturbed Stark manifolds. An example of destructive interference can be seen to the high-energy side of the $n'=8$ perturber manifold in Figs. 4 and 5(a), where the underlying Stark states have decreased intensity relative to the unperturbed manifolds. This perturbation is a weak series perturbation in the sense that the perturber identity is not lost and the dominant effect is the asymmetric redistribution of oscillator strength in the vicinity of the perturber [22]. This effect can be seen clearly in the oscillator strengths of the experimental absorption map at the avoided crossings, which measure the interaction between the Rydberg electron and the ion core. Figure 5(a) focuses on the $8f'$ perturbation's influence on the avoided crossings. The oscillator strengths are enhanced near the perturbation, especially on the high-energy side of the avoided crossings. For comparison Fig. 5(b) shows an unperturbed region of the absorption map over the same scaled-energy range with an effective-principal-quantum-number range higher by 2.

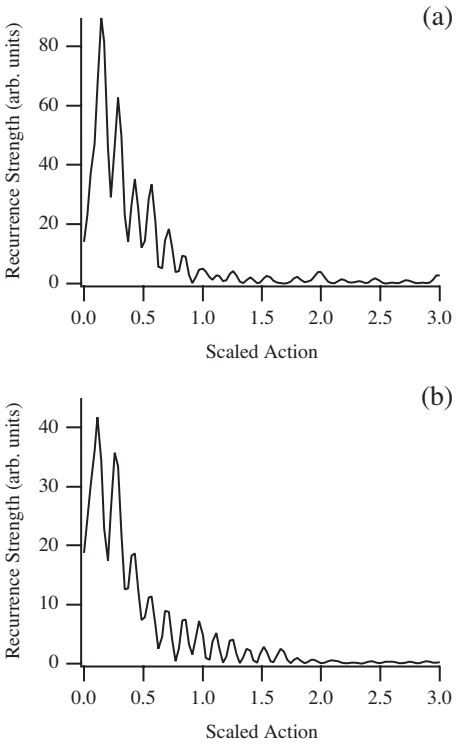

FIG. 7. Recurrence spectra at low scaled actions for (a) $\varepsilon=-3.175$ and (b) $\varepsilon=-2.3$.

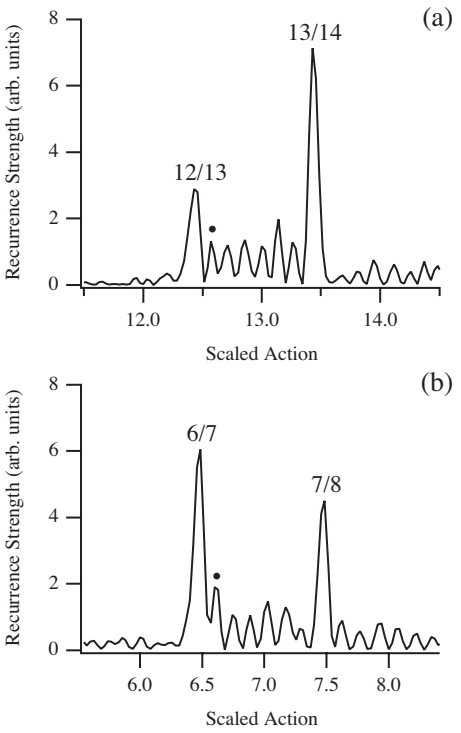

FIG. 8. Recurrence spectra at scaled actions in the vicinity of the first band of closed-classical-orbit peaks for (a) $\varepsilon=-3.175$ and (b) $\varepsilon=-2.3$. Six peaks associated with core-changing collisions are present between the two closed-orbit peaks, and one is identified by a dot (see text).

C. Observations of Stark recurrence spectra

Figure 6 shows the Stark recurrence map obtained by Fourier transforming the absorption spectra shown in Fig. 2 for scaled energies ranging from −3.5 to −2. We discuss two distinct features in the recurrence map of Fig. 6 that result from the perturbations.

The interval between the perturbers in the absorption spectrum is much larger than the average spacing of states in the principal Rydberg series so that the Fourier transform produces recurrence peaks with scaled actions of less than 1, the smallest scaled action of a peak in the recurrence spectrum of a regular hydrogenic series. To show this effect in more detail, Fig. 7 shows two spectra of the recurrence map shown in Fig. 6, at scaled energies of −3.175 and −2.3 and scaled action ranging from 0 to 3.0. We observe seven peaks at scaled actions less than or equal to 1. The first peak has a scaled action of 1/7 (0.14). The other peaks occur at integer multiples of this primary scaled action. The uncertainty in location of the peaks (0.05) arises from the finite range of effective principal quantum number investigated in the absorption spectrum. The peaks form a series with the first peak being the primitive and successive peaks being repetitions. The series of recurrence peaks results from the pair of perturbations in the absorption spectrum which are spaced on the n^* scale by an interval of approximately 7, that is, the inverse of 0.14. As a result, we call members of this series "perturber-pair recurrences." The primitive perturber-pair recurrence has the greatest intensity and its repetitions monotonically decay.

We now discuss how a pair of perturbations in the absorption spectrum affects the recurrence spectrum at higher scaled action just above the downhill-orbit-bifurcation point of the first band of closed classical orbits [10]. Figure 8 shows two spectra of the recurrence map shown in Fig. 6 with scaled energies of −3.175 in panel (a) and −2.3 in panel (b). The scaled-action ranges of 11.5–14.5 in panel (a) and 5.5 to 8.5 in panel (b) are chosen to be in the vicinity of the first band of bifurcated closed classical orbits [10] which are labeled in Fig. 8 by the orbital period ratios [7]. The argon recurrence spectrum shows two large peaks corresponding to closed classical single-electron orbits. In between those peaks, the recurrence spectrum shows a series of additional peaks that do not exist in an unperturbed spectrum. The additional peaks occur at scaled actions of $S'_{co}+k/7$, where S'_{co} is the scaled action of the lower-scaled-action closed classical orbit (6/7,12/13) and $k=1,2,\ldots,6$. These additional peaks are not simply repetitions of the primitive recurrence.

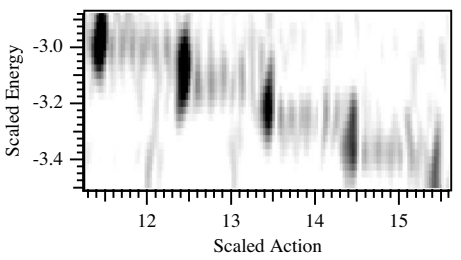

FIG. 9. Stark recurrence map in the vicinity of $\varepsilon=-3.175$ illustrating strong and weak recurrence regions to the right and left of the closed-classical-orbit dark regions.

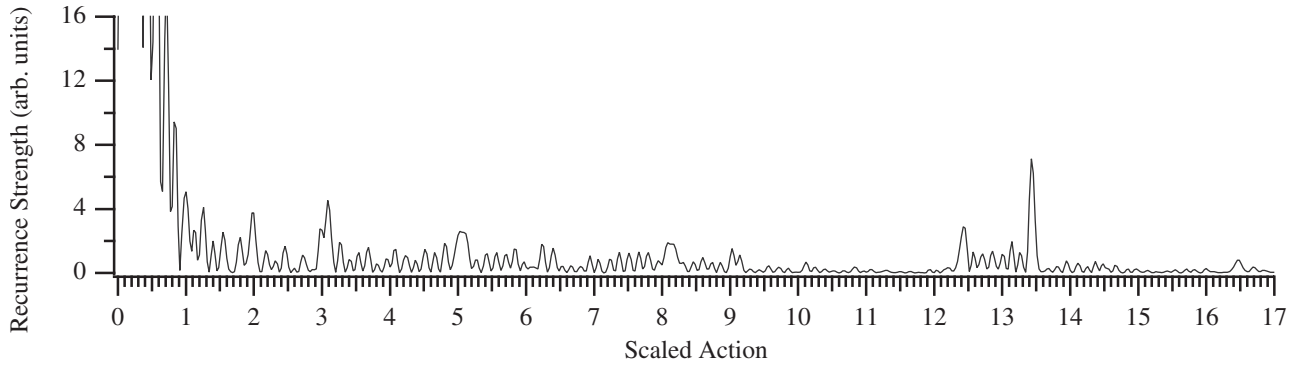

FIG. 10. Recurrence spectrum at $\varepsilon=-3.175$ over the scaled-action range of 0–17.

To illustrate this point, Fig. 9 shows several spectra of the recurrence map in the vicinity of $\varepsilon=-3.175$, showing the absence of peaks on the low-action side of the classical-orbit peaks and strong-signal peaks between adjacent classical-orbit peaks. Finally, we show in Fig. 10 an expanded scaled-action view of the −3.175 scaled-energy recurrence spectrum. The repetitions of the primitive perturber-pair recurrence peak have decayed away by a scaled action of ~11.

To emphasize the fact that the effects described above do not occur in the Stark recurrence spectra of a regular [23] Rydberg series of argon, i.e., a series containing no interlopers, we show in Fig. 11 the measured Stark recurrence map [24] for the autoionizing Rydberg series converging to the $^2P_{1/2}$ ionization threshold. (A plot of the measured absorption map associated with the recurrence map shown in Fig. 11 can be found in Ref. [25].) The recurrence map is very clean in comparison to Fig. 6 and shows no sign of the multielectron effects discussed above.

III. DISCUSSION AND CONCLUSION

We now discuss a physical picture associated with the two observed effects in the measured recurrence spectrum. Although the details of the short-range dynamics differ, the physical picture is similar to that presented by Matzkin *et al.* [26,27] in a theoretical semiclassical investigation of the hydrogen molecule in a magnetic field and described in their experimental investigation of the NO molecule in a magnetic field [28]. Recent theoretical work on inelastic scattering in helium in a magnetic field is also relevant [29].

As described in Sec. II, the recurrence peaks below $S'=1$ result from the $n'=8$ and 10 perturbations in the absorption spectrum, they do not appear in the recurrence spectra of atomic hydrogen, and they do not appear in the regular spectrum of autoionizing Rydberg Stark states of argon. The $n'=8$ and 10 perturbers are members of the Rydberg series associated with an excited state of the ion core, $3p^5(^2P_{1/2})$. For these reasons, we associate the new recurrences in the spectrum below $S'=1$ with the dynamics of a Rydberg electron coupled to the $^2P_{1/2}$ angular momentum state of the ionic core. It is important to note that the perturbers in the absorption spectrum belong to a nonscaled Rydberg series and have different orbital angular momenta associated with the ionic core. Consequently, the peaks in the recurrence spectrum do not have a direct correspondence with simple classical Kepler orbits of a Rydberg electron orbiting an excited ion core. They represent a more complicated radial and angular motion, the details of which extend beyond the scope of the present work. We simply note that the first peak at $S'=0.14$ is the primitive recurrence of the perturber pair with additional peaks at multiples of 0.14 due to repetitions of the fundamental motion associated with the perturber pair.

It is well known in the field of recurrence spectroscopy that combination orbits due to elastic scattering of the Rydberg electron with the ion core are present in nonhydrogenic atomic systems [7,30]. The combination orbits produce

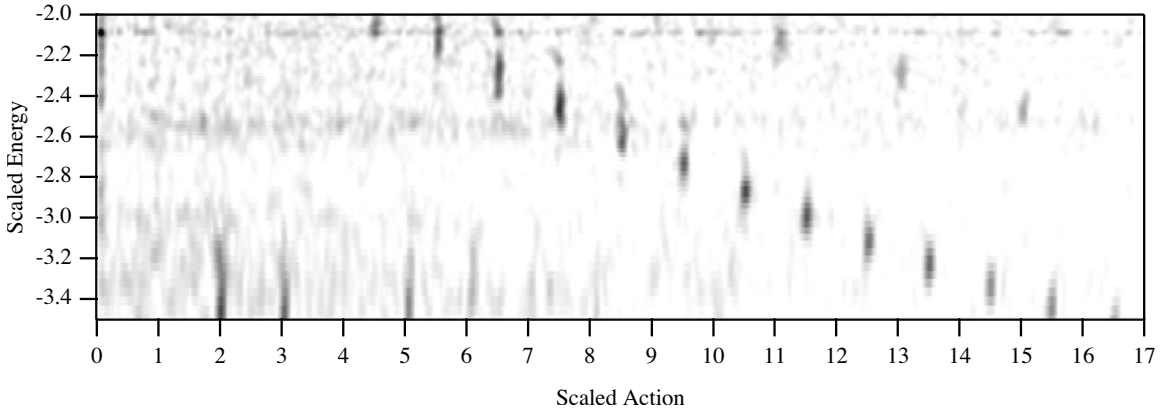

FIG. 11. Measured Stark recurrence map of argon as a function of scaled energy and scaled action S''.

peaks in the recurrence spectrum that occur at the sum of the scaled actions associated with hydrogenic orbits. Inelastic scattering is also possible under certain circumstances [26]. In this context, we address the appearance of the recurrence peaks observed between the closed-classical-orbit recurrences as shown in Figs. 8–10. Each peak occurs at the sum of the scaled action of the nearest lower-action hydrogenic closed classical Stark orbit and the primitive perturber-pair recurrence (or one of its repetitions). Semiclassically, these peaks represent inelastic collisions between the Rydberg electron and the ion core. For example, the laser excites an outgoing Rydberg electron that executes the 6/7 or 12/13 Stark orbit with scaled action of 6.5 or 12.5 (see Fig. 8), returns to the core, undergoes an inelastic-scattering event, leaves the core excited, and executes a motion with scaled action of 0.14, producing peaks in the recurrence spectrum at 6.64 and 12.64, the sum of the two scaled actions. The resulting inelastic combination recurrence peaks are identified in Fig. 8 by a dot in each spectrum. The next five peaks to the right of the dotted peak are recurrences that occur due to inelastic collisions between the closed classical orbit and a repetition of the fundamental motion of the primitive perturber pair.

In conclusion, we have measured and discussed the Stark scaled-energy photoabsorption spectrum and the associated recurrence spectrum of the argon atom in a uniform electric field in a region where Rydberg states interact with two different configurations ($^3P_{3/2}$ and $^2P_{1/2}$) of the ion core. We have observed other types of peaks in the recurrence spectrum due to the perturbers and interpreted them. One type of recurrence peak is associated with a Rydberg electron orbiting an excited atomic-ion core. The other type of recurrence peak results from the Rydberg electron inelastically scattering between configurations in which the ionic core has angular momentum $j_c=1/2$ or 3/2. In addition, we observe higher-order inelastic-scattering recurrence peaks resulting from core-changing collisions between a closed orbit of the Rydberg electron and a repetition of a primitive recurrence of the perturber pair.

ACKNOWLEDGMENTS

We wish to acknowledge the National Science Foundation for support of this work and Josh H. Gurian and Marcus van-Lier Walqui for assistance in the laboratory.

[1] M. L. Du and J. B. Delos, Phys. Rev. A **38**, 1896 (1988).
[2] M. L. Du and J. B. Delos, Phys. Rev. A **38**, 1913 (1988).
[3] J. Gao and J. B. Delos, Phys. Rev. A **46**, 1455 (1992).
[4] R. Blümel and W. P. Reinhardt, *Chaos in Atomic Physics* (Cambridge University Press, Cambridge, England, 1997).
[5] S. N. Pisharody, J. G. Zeibel, and R. R. Jones, Phys. Rev. A **61**, 063405 (2000).
[6] U. Eichmann, K. Richter, D. Wintgen, and W. Sandner, Phys. Rev. Lett. **61**, 2438 (1988).
[7] M. Courtney, N. Spellmeyer, H. Jiao, and D. Kleppner, Phys. Rev. A **51**, 3604 (1995), and references therein.
[8] A. Kips, W. Vassen, and W. Hogervorst, J. Phys. B **33**, 109 (2000), and references therein.
[9] X. J. Liu, J. W. Cao, M. S. Zhan, and J.-P. Connerade, J. Phys. B **35**, 2069 (2002), and references therein.
[10] M. L. Keeler, H. Flores-Rueda, J. D. Wright, and T. J. Morgan, J. Phys. B **37**, 809 (2004), and references therein.
[11] R. V. Jensen, H. Flores-Rueda, J. D. Wright, M. L. Keeler, and T. J. Morgan, Phys. Rev. A **62**, 053410 (2000).
[12] K. A. Bates, J. Masae, C. Vasilescu, and D. Schumacher, Phys. Rev. A **64**, 033409 (2001).
[13] J. Murray-Krezan, J. Kelly, M. R. Kutteruf, and R. R. Jones, Phys. Rev. A **75**, 013401 (2007).
[14] In the present work the presence or absence of a prime in the notation of a quantum state indicates 3/2 or 1/2 for the total angular momentum of the ion core.
[15] M. Keeler and T. J. Morgan, Phys. Rev. Lett. **80**, 5726 (1998).
[16] T. F. Gallagher, *Rydberg Atoms* (Cambridge University Press, Cambridge, England, 1994).
[17] P. M. Koch and D. R. Mariani, Phys. Rev. Lett. **46**, 1275 (1981).
[18] In this case, the scaled energy is defined as $\varepsilon'=E'F^{-1/2}$, where E' is the electron binding energy measured relative to the $^2P_{1/2}$ ionization limit. For a scaled energy of ε the scaled energy for the $^2P_{1/2}$ series is $\varepsilon'=(n^*/n^{*\prime})^{-2}\varepsilon$, where $n^{*\prime}=(-2E')^{-1/2}$.
[19] J. D. Wright, T. J. Morgan, L. Li, Q. Gu, J. L. Knee, I. D. Petrov, V. L. Sukhorukov, and H. Hotop, Phys. Rev. A **77**, 062512 (2008).
[20] I. Petrov, T. Peters, T. Halfmann, S. Aloise, P. O'Keeffe, M. Meyer, V. Sukhorukov, and H. Hotop, Eur. Phys. J. D **40**, 181 (2006).
[21] M. Pellarin, J. L. Vialle, M. Carre, J. Lerme, and M. Aymar, J. Phys. B **21**, 3833 (1988).
[22] A. W. Weiss, Phys. Rev. A **9**, 1524 (1974).
[23] The autoionization widths (addressed in a separate paper) will not change any of the conclusions drawn here.
[24] Each spectrum in the recurrence map derives from a constant scaled energy, $\varepsilon'=E'F^{-1/2}$, absorption spectrum that is Fourier transformed with respect to the effective principal quantum number $n^{*\prime}=(2E')^{-1/2}$, where E' is the Rydberg-electron binding energy measured relative to $^2P_{1/2}$ ionization threshold, to obtain the recurrence strength as a function of scaled action S''.
[25] L. Li, Q. Gu, J. L. Knee, J. D. Wright, J. M. DiSciacca, and T. J. Morgan, J. Opt. Soc. Am. B **25**, 334 (2008).
[26] A. Matzkin and T. S. Monteiro, Phys. Rev. Lett. **87**, 143002 (2001).
[27] A. Matzkin, P. A. Dando, and T. S. Monteiro, Phys. Rev. A **66**, 013410 (2002).
[28] A. Matzkin, M. Raoult, and D. Gauyacq, Phys. Rev. A **68**, 061401(R) (2003).
[29] L. B. Zhao and M. L. Du, Phys. Lett. A **363**, 453 (2007).
[30] M. L. Keeler and T. J. Morgan, Phys. Rev. A **59**, 4559 (1999).